

ORIGINAL ARTICLE

AP-3 complex subunit delta gene, *ap3d1*, regulates melanogenesis and melanophore survival via autophagy in zebrafish (*Danio rerio*)

Sam J. Neuffer¹ | David Beltran-Cardona² | Kevin Jimenez-Perez² | Lauren F. Clancey² | Alexander Brown² | Leslie New^{2,3} | Cynthia D. Cooper^{1,2}

¹School of Molecular Biosciences, Washington State University Vancouver, Vancouver, WA, USA

²College of Arts and Sciences, Washington State University Vancouver, Vancouver, WA, USA

³Department of Mathematics and Computer Science, Ursinus College, Collegeville, Pennsylvania, USA

Correspondence

Cynthia D. Cooper, School of Molecular Biosciences, Washington State University Vancouver, Vancouver, WA, USA.
Email: cdcooper@wsu.edu

Funding information

Washington State University Vancouver; National Institutes of Health; Washington State University

Abstract

Zebrafish are an emerging model organism to study the syndromic albinism disorder, Hermansky-Pudlak syndrome (HPS), due to visible pigment development at 24 hours postfertilization, and conserved melanogenesis mechanisms. We describe *crasher*, a novel HPS type 10 (HPS10) zebrafish model, with a mutation in AP-3 complex subunit delta gene, *ap3d1*. Exon 14 of *ap3d1* is overexpressed in *crasher* mutants, while the expression of *ap3d1* as a whole is reduced. *ap3d1* knockout in *AB zebrafish recapitulates the mutant *crasher* phenotype. We show *ap3d1* loss-of-function mutations cause significant expression changes in the melanogenesis genes, dopachrome tautomerase (*dct*) and tyrosinase-related protein 1b (*tyrp1b*), but not tyrosinase (*tyr*). Last, Generally Applicable Gene-set Enrichment (GAGE) analysis suggests autophagy pathway genes are upregulated together in *crasher*. Treatment with autophagy-inhibitor, bafilomycin A1, significantly decreases melanophore number in *crasher*, suggesting *ap3d1* promotes melanophore survival by limiting excessive autophagy. *crasher* is a valuable model to explore the regulation of melanogenesis gene expression and pigmentation disease.

KEYWORDS

albinism, cell survival, differentiation, Hermansky-Pudlak syndrome, specification

1 | INTRODUCTION

DNA-damaging ultraviolet (UV) radiation from the sun is absorbed by the black pigment, melanin (Herrling et al., 2008). Mammalian melanocyte cells produce melanin during melanogenesis. Melanogenesis depends upon multiple enzymes. Microphthalmia transcription factor (MITF) controls tyrosinase (TYR), tyrosinase-related protein 1 (TYRP1), and dopachrome tautomerase (DCT) expression (Kawakami & Fisher, 2017). The latter three enzymes

convert tyrosine into melanin (Pillaiyar et al., 2017). Melanogenesis is an adaptive, conserved process regulated by homologous genes across animal taxa (Hoekstra, 2006).

Dysfunctional melanogenesis causes the heterogenic disorder, albinism (Garrido et al., 2021). People with albinism have visual impairments and increased skin cancer risk (Inena et al., 2020; Izquierdo et al., 1995). Albinism can be caused by defects in melanocyte specification and differentiation or can be non-syndromic or syndromic (Federico & Krishnamurthy, 2020;

This is an open access article under the terms of the [Creative Commons Attribution-NonCommercial-NoDerivs](https://creativecommons.org/licenses/by-nc-nd/4.0/) License, which permits use and distribution in any medium, provided the original work is properly cited, the use is non-commercial and no modifications or adaptations are made.

© 2022 The Authors. *Pigment Cell & Melanoma Research* published by John Wiley & Sons Ltd.

Pingault et al., 2010). Non-syndromic albinism disorders, such as Oculocutaneous Albinism 2 (*Oca2*), result from mutations in melanogenesis enzymes and proteins supporting melanogenesis enzyme function (Federico & Krishnamurthy, 2020; Garrido et al., 2021; Park et al., 2015; Wang et al., 2019). Syndromic albinism, such as Hermansky–Pudlak syndrome (HPS), results from mutations pertaining to lysosome-related organelle (LRO) function (Ammann et al., 2016; Federico & Krishnamurthy, 2020; Mohammed et al., 2019). HPS10 is caused by mutations in the adaptor protein 3 (AP-3) complex subunit delta gene, *AP3D1*, important for trafficking tyrosinase to the LROs, melanosomes (Ammann et al., 2016; Mohammed et al., 2019; Richmond et al., 2005). HPS10 patients suffer from symptoms related to defects in LRO function such as seizures (neurotransmitter release) and recurrent infections due to reduced natural killer cell function (granule release), resulting in a short life expectancy (Ammann et al., 2016; Mohammed et al., 2019). The rarity of HPS10 begets a paucity of research of the disease.

Zebrafish are excellent models for studying albinism due to visible pigment development at 24 hours postfertilization (hpf) and conserved melanogenesis and melanophore (melanocytes in mammals) development pathways (Braasch et al., 2007; Kimmel et al., 1995). Here, we describe *crasher*; an albino mutant zebrafish with unusual single-exon overexpression and reduced expression of *AP3D1* homolog, *ap3d1*, and HPS10-like symptoms. We found *ap3d1* knockout recapitulates the *crasher* phenotype, and melanophores specified and differentiated correctly in *ap3d1* mutant zebrafish. *crasher* provides novel information, including decreased *dct* and *tyrp1b* expression with *ap3d1* loss-of-function. Finally, inhibiting autophagy with bafilomycin A1 negatively impacted melanophore survival, most significantly in *crasher* mutant larvae.

2 | METHODOLOGY

2.1 | Ethics statement

Research protocols using animals and recombinant DNA/RNA are approved by the Washington State University Institutional Animal Care and Use Committee (ASAF 3848 and 6777) and the Institutional Biosafety Committee (BAF 1107).

2.2 | Fish husbandry

Fish were fed dry and live foods, maintained on a recirculating water system at 28–30°C on a 14-h light/10-h dark cycle and checked daily for abnormal behavior. *AB zebrafish are a wild-type strain. The *crasher* mutant allele was maintained in heterozygous adults. *oca2* were also maintained as heterozygotes (Beirl et al., 2014). Embryos were raised in E3 embryo media (EM) at 28°C (Westerfield, 2007). Embryos were staged according to Kimmel et al. (1995).

Significance

We have characterized a new zebrafish model for Hermansky-Pudlak syndrome type 10. Using this model, we have shown *ap3d1* is important for melanophore survival via autophagy. This model can be used to better understand the molecular mechanisms of disease in HPS10 and AP-3 complex function.

2.3 | Isolation and mapping of *crasher*

crasher originated from an ENU mutagenesis screen at Steve Johnson's Laboratory (Washington University). The *crasher* mutation was mapped to chromosome 22 from larvae at 3 days post-fertilization (dpf) via bulk segregant and fine mapping analysis described previously (Clancey et al., 2013). See [Methods S1](#).

2.4 | Clustered regularly interspaced short palindromic repeats (CRISPR) gene knockout

Two CRISPR guide DNA oligos per candidate gene were designed using CRISPR scan (Moreno-Mateos et al., 2015). Highest-scoring guides were selected if they targeted an early exon with no predicted off-targets. Guides were annealed to Cas9 interacting scaffold (gatccgcaccgactcggtgccactttttcaagttgataacggactagccttatttacttgctatttctagctctaaac). Guide RNA (gRNA) was synthesized then purified and injected into embryos at the 1–2 cell stage. Detailed description in [Methods S1](#). Embryos at 3 dpf were fixed in 4% paraformaldehyde (PFA; Sigma-Aldrich) overnight at 4°C. Experiments replicated three times.

2.5 | *In situ* hybridization

Embryos at 24 and 30 hpf were dechorionated, fixed in 4% PFA for 6 hours at room temperature, and dehydrated and stored in methanol at –20°C until used. *In situ* hybridization protocol was derived from Thisse et al., 1993 with modifications (Thisse et al., 1993). No proteinase K was used. Hybridization and washes were performed at 65°C. Digoxigenin-labeled probes for *foxd3* (Odenthal & Nusslein-Volhard, 1998), *mitfa* (Lister et al., 1999), *dct* (Kelsh et al., 2000), *tyr* (Camp & Lardelli, 2001), and *tyrp1b* (Braasch et al., 2009), were previously described. Experiments replicated three times unless otherwise stated.

2.6 | Bafilomycin A1 autophagy drug treatments

2.5 dpf *crasher* mutant and wild-type (WT) sibling larvae were treated with 50nM bafilomycin A1 (Enzo Life Sciences) in EM containing 1%

dimethylsulfoxide (DMSO) (Sigma-Aldrich) or with 1% DMSO in EM as a control. Each day, 50% of treatment solution was replaced with fresh EM/DMSO solution with or without drug. At 5 dpf, fish were fixed in 4% PFA. Experiments replicated four times.

2.7 | Imaging

Fish were visualized and imaged under a Nikon SMZ1500 microscope and a Digital Sight DSRI1 camera. Live fish were anesthetized with tricaine (Western Chemical Inc) and transferred to an EM droplet with methylcellulose on a glass slide. After imaging, fish recovered in fresh EM. Fixed CRISPR and bafilomycin A1 experiment fish were imaged in 50% glycerol/PBS on a glass slide. Fixed *in situ* experiment fish were imaged in 50% glycerol/PBS using a bridged coverslip. Images were white balanced and cropped using Adobe Photoshop Elements 2020.

2.8 | Cell counts

Cells were counted under a Nikon SMZ1500 microscope. For *crasher* mutant and CRISPR-edited fish, melanophores were counted throughout the body. For *in situ* cell counts, *in situ* signal+ cells were counted over the whole body (except eyes). The dorsal stripe melanophores were counted looking top-down, and ventral stripe melanophores were counted on one side of bafilomycin A1-treated fish. The dorsal and ventral stripe signal were counted by observing the fish ventrally for the *mitfa*+ 30 hpf dorsal/ventral ratio *in situ*. Experiments replicated three times unless otherwise stated. Statistical analyses were performed using the packages dev.tools (v2.3.2; Wickham et al., 2020), tidyverse (Wickham et al., 2019), rstatix (v.0.7.0; Kassambara,

2021), car (Fox & Weisberg, 2019), nortest (v1.0-4; Gross & Ligges, 2015) and R base packages (v.4.0.4; R Core Team, 2021).

2.9 | RNA-Seq and quantitative reverse transcription PCR (qRT-PCR)

2.9.1 | Sample preparation and sequencing

Three samples each of 50 *crasher* homozygous recessive mutants and 50 *AB line fish were collected at 3 dpf and stored at -80°C in TRIzol (ThermoFisher Scientific). RNA was extracted and single-end sequenced using an HiSeq3000 (Illumina, HiSeq) at a read length of 100 bp at Oregon State University's Center for Genome Research and Biocomputing (Corvallis, OR). Detailed description in [Methods S1](#).

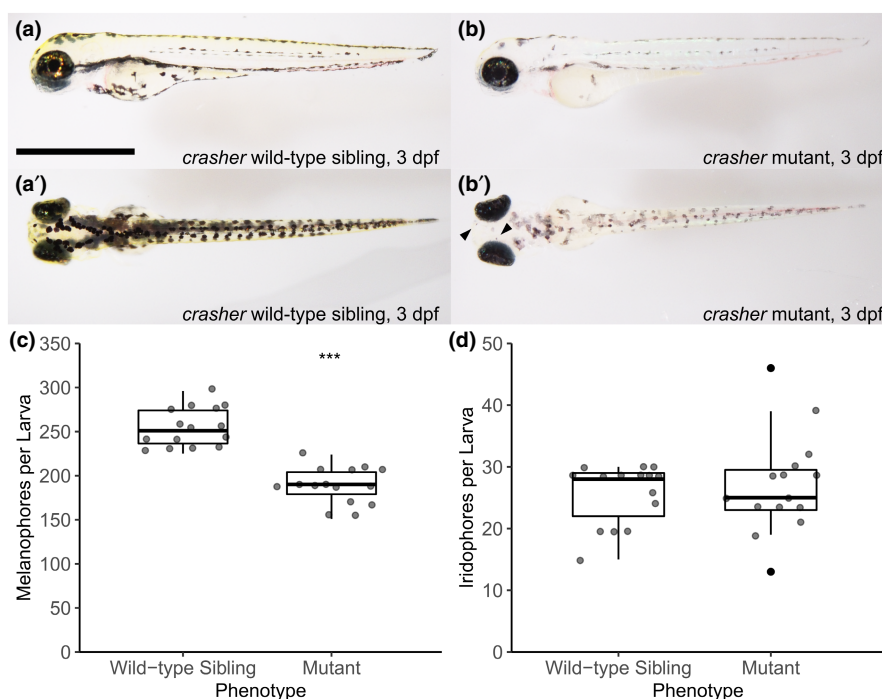
2.9.2 | Data preparation

Sequencing quality was determined using FASTQC and adaptor sequences trimmed using Trimmomatic (Andrews, 2019; Bolger et al., 2014). Genome alignment and indexing to Ensembl *Danio rerio* genome version 99 was performed using STAR to create a sequence alignment map (SAM) file (Dobin et al., 2013; Yates et al., 2020).

2.9.3 | RNA-Seq data analysis

STAR alignment was performed to generate gene counts using R then converted into Transcripts Per Million. Generally Applicable Gene-set Enrichment (GAGE) for pathway analysis was performed

FIGURE 1 *crasher* mutants have fewer and lighter melanophores. (a, a') Lateral (a) and dorsal (a') view of *crasher* siblings with typical the wild-type (WT) phenotype at 3 days postfertilization (3 dpf). (b, b') Lateral (b) and dorsal (b') view of homozygous recessive (mutant) phenotype. Arrowheads indicate punctate melanophores. (c) Melanophore count boxplot at 3 dpf. Mutants average 25% fewer melanophores ($\mu = 188$, $\text{SD} = 20.4$) than WT siblings ($\mu = 255$, $\text{SD} = 20.9$). (Student's *t*-test, $t[28] = -8.87$, $p = 1.27 \times 10^{-9***}$). (d) Iridophore count boxplot at 3 dpf. Mutants vary more (median = 25, interquartile range [IQR] = 23 to 29.5), but have similar iridophore numbers as WT siblings (median = 28, IQR = 22–29) (Mann–Whitney U test, $W = 11.05 \times 10^4$, $p = 0.95$). Scale bar is 1 mm.



in R (Luo et al., 2009; Luo & Brouwer, 2013; R Core Team, 2021; Yates et al., 2020). Single-gene expression data was called using the median value within 3 samples per genotype for each gene using the BiomaRt package (Durinck et al., 2005).

SAM files were compressed into binary alignment map (BAM) files using SAMtools (Li et al., 2009). Mutations were called using somatic calling in VarScan2 with *AB fish defined as “normal” and *crasher* mutants or *oca2* homozygous recessive mutants defined as “tumor” (Koboldt et al., 2012).

Exon read counts for each candidate gene were normalized to RPKM and read ratios between *AB and *crasher* mutants determined

by dividing normalized *crasher* read number at each exon by normalized *AB read number at each exon.

2.9.4 | Quantitative Reverse Transcription PCR (qRT-PCR)

qRT-PCR was performed to quantify *ap3d1* transcripts as detailed in the Methods S1. Transcripts were normalized to *actb1* as a reference gene using the Pfaffl method (Pfaffl, 2001). Statistical analyses were performed using the packages dev.tools (v2.3.2; Wickham et al.,

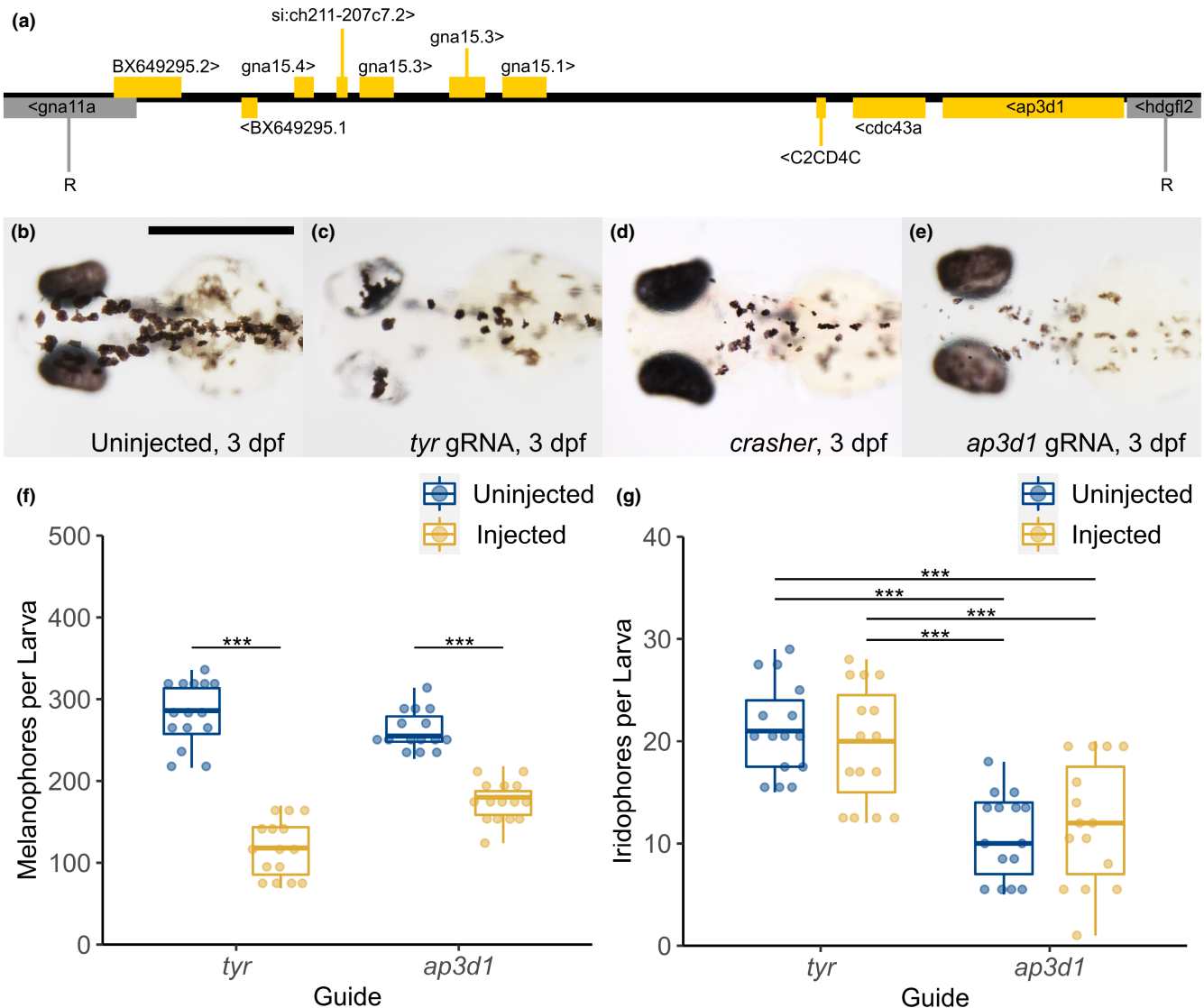


FIGURE 2 *crasher* mutant phenotype recapitulation using CRISPR knockout. (a) The *crasher* mutation maps to a ~375 kb region on chromosome 22. R = recombination event. (b–g) CRISPR *ap3d1* knockout in *AB lines recapitulates the *crasher* phenotype. (b) Uninjected *AB control. (c) *tyr* gRNA injected *AB fish have mosaic tyrosinase activity. (d) *crasher* mutant with slight lightening of the retinal pigmented epithelium. (e) *ap3d1* gRNA injected *AB fish display light, punctate *crasher*-like melanophores and a lighter retinal pigmented epithelium than *crasher* mutant. (f) Melanophore count boxplot in uninjected and injected *tyr* and *ap3d1* fish. Melanophore number is reduced in both populations injected with gRNA (two-way ANOVA, guide $F(1, 56) = 5.50, p = <0.02$; injection status $F(1, 56) = 247.50, p = <0.22 \times 10^{-15}$; interaction $F(1, 56) = 23.68, p = <9.68 \times 10^{-6}$, Tukey HSD performed to determine group differences, $p = <0.001^{***}$). (g) Boxplot shows iridophore number is unchanged between uninjected and injected for both guides (two-way ANOVA, injection status $F(1, 56) = 0.02, p = 0.88$; guide $F(1, 56) = 46.05, p = 7.80 \times 10^{-9}$; interaction $F(1, 56) = 0.89, p = 0.35$, Tukey HSD performed to determine group differences, $p = <0.001^{***}$). Scale bar is 500 μm . 78 eggs injected for *tyr*; 58 eggs injected for *ap3d1*.

2020), tidyverse (Wickham et al., 2019), rstatix (v.0.7.0; Kassambara, 2021), car (Fox & Weisberg, 2019), and R base packages (v.4.0.4; R Core Team, 2021).

3 | RESULTS

3.1 | *crasher* homozygous recessive mutants have fewer and lighter melanophores

The *crasher* phenotype is discerned at 2.5–3 days postfertilization (dpf), and inherited in a single-gene, autosomal recessive pattern. Similar to mocha mouse melanocytes, melanophores were lighter, indicative of a melanin synthesis problem (Figure 1a–b'; Kantheti et al., 1998). Some mutant melanophores appear punctate. Total melanophore number was significantly reduced at 3 dpf in mutants when compared to their wild-type (WT) siblings (Figure 1c). Interestingly, mutants appear to have less yellow pigment (Figure 1a–b'). Silver iridophore number was unchanged at 3 dpf (Figure 1d). Mutants were lethargic and survived ~9–11 dpf. The observed albinism and early-death phenotype is shared with HPS10 patients (Ammann et al., 2016; Mohammed et al., 2019).

3.2 | CRISPR *ap3d1* knockout recapitulates the mutant phenotype and *crasher* mutants overexpress exon 14 in *ap3d1*

crasher mutation mapping analysis revealed several “candidate genes” (Figure 2a). Only AP-3 complex subunit delta 1 (*ap3d1*) is associated with albinism (Ammann et al., 2016; Kantheti et al., 1998; Mohammed et al., 2019). We hypothesized disrupting *ap3d1* function via CRISPR within wild-type *AB zebrafish could recapitulate the *crasher* phenotype by disrupting melanogenesis enzyme cargo transport to the melanosome (Richmond et al., 2005). Positive control CRISPR *tyrosinase* guide injection caused pigment loss (Figure 2c). *ap3d1* guide injection recapitulated lighter and punctate *crasher*-like melanophores (Figure 2d,e). A two-way ANOVA tested injection status (injected or uninjected) and guide type (*ap3d1* or *tyr*) main effects on melanophore number, and were statistically significant, as was the interaction effect. A *post hoc* Tukey's Honest Significant Difference (HSD) test showed differences between uninjected and injected melanophore counts for both guide types were statistically significant (Figure 2f; Table S1). Two additional replicates were analyzed by two-factor permutations to handle unequal variance between treatment groups (Howell, 2009). Injection status was always significant. Guide and interaction effects were inconsistent across replicates (Table S2).

Iridophore counts were analyzed via two-way ANOVA in fish injected with *tyr* or *ap3d1* guide (Figure 2g). Guide type main effect was statistically significant, but not injection status and interaction effects. Iridophore number was significantly reduced between

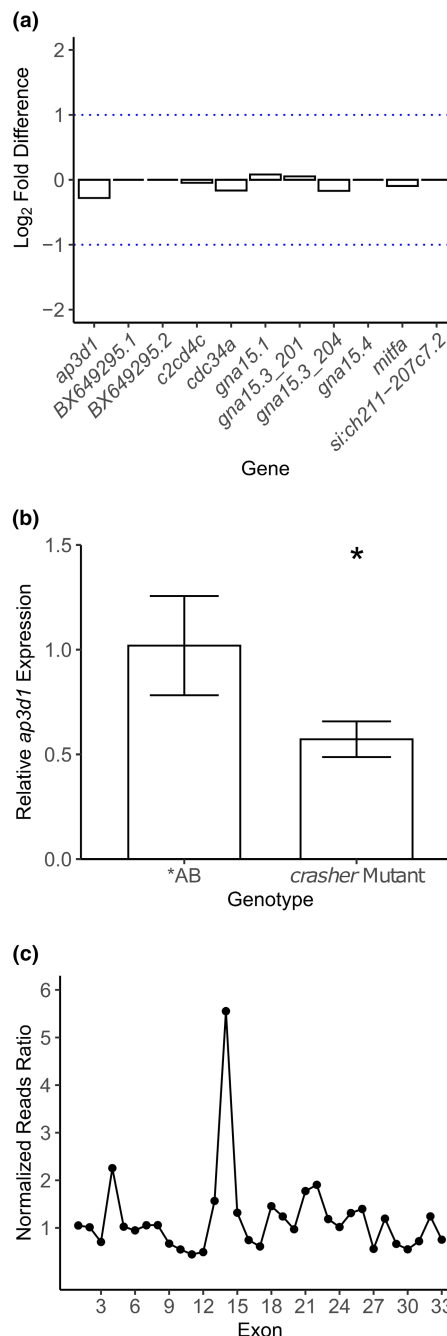


FIGURE 3 *ap3d1* gene expression is reduced overall in *crasher* mutants, but exon 14 of *ap3d1* is overexpressed. (a) RNA-Seq data bar graph shows no reduction in any candidate gene in *crasher* mutants as compared to *AB to a log₂ fold difference of 1. Log₂ fold difference is the difference in mutant and *AB expression. However, *ap3d1* expression is reduced the most. Negative values indicated reduced expression in *crasher* mutants as compared to *AB. A difference of 1 is considered of import and equivalent to a twofold difference. Significance testing was not performed. (b) *ap3d1* expression is reduced in *crasher* mutants according to qRT-PCR (Student's *t*-test, $t[4] = 2.94$, $p = 0.04^*$, $n = 3$). Error bars are standard deviation. (c) Exon 14 overexpression in *ap3d1* line graph. The normalized reads ratio is defined as the normalized (transcripts per million) number of *crasher* reads at that exon divided by the normalized number of *AB reads at that exon.

embryos injected with *ap3d1* or *tyr* guide. However, *ap3d1* guide injection did not reduce iridophore number compared to uninjected siblings (Table S3). Injection status effects were not significant in three replicates. Notably, iridophore development was not affected by *ap3d1* knockouts, which is an expected finding as iridophore development is not affected in *crasher* mutants at 3 dpf.

VarScan analysis compared nucleotides at each position in the *AB wild-type line and *crasher* mutant line in the exome of candidate genes, but did not reveal a strong candidate causing the mutant phenotype (Table S4). We asked if candidate gene expression changed in *crasher* mutants. Since we performed RNA-Seq in whole larvae, we included *mitfa* expression to rule out changes due to reduced numbers of

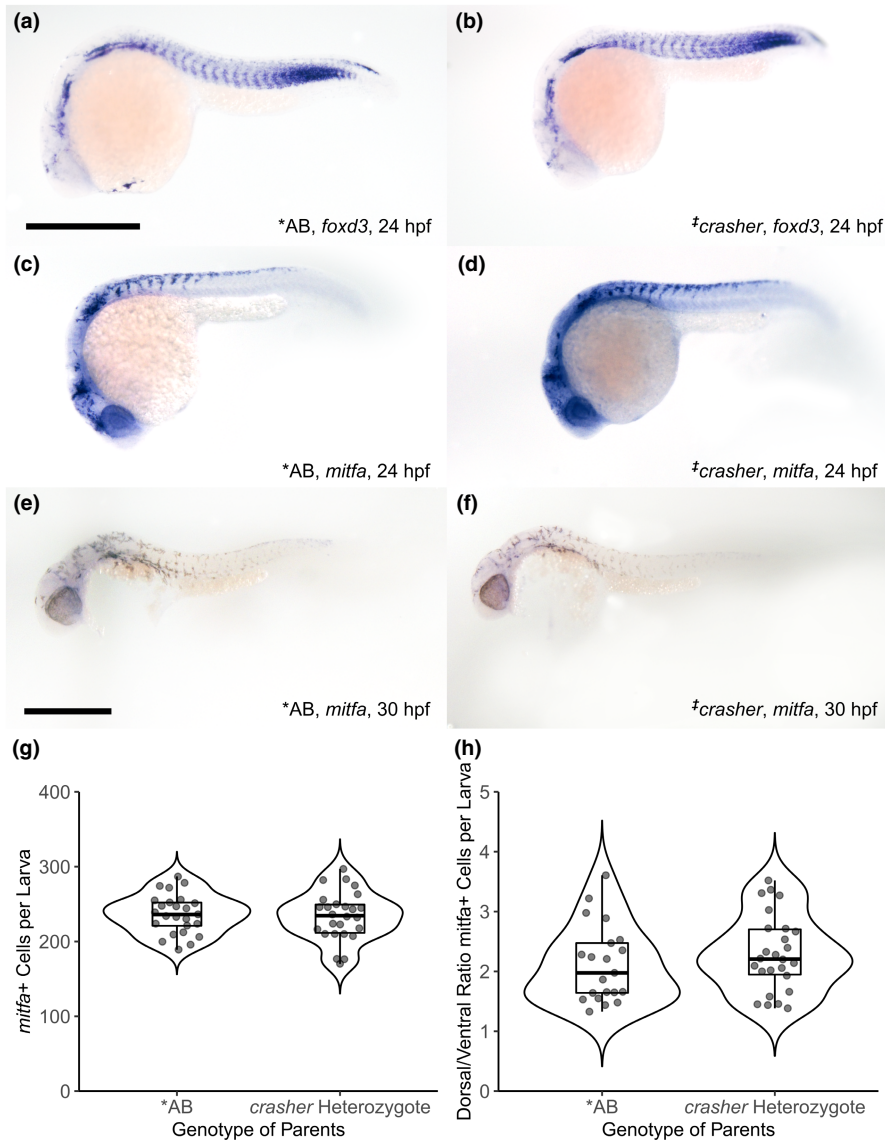
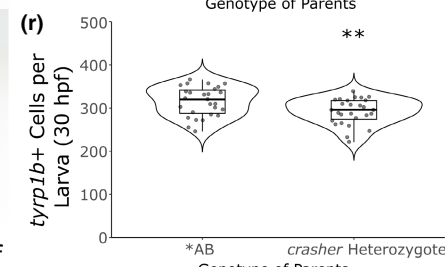
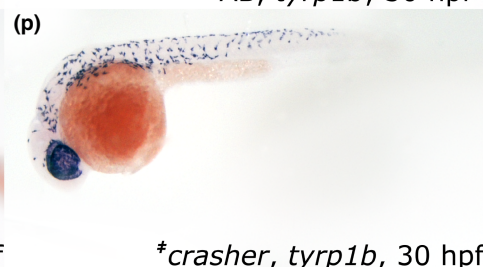
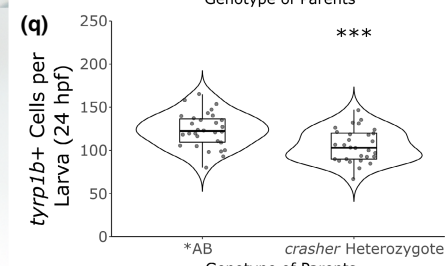
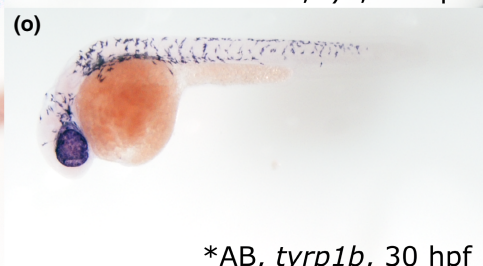
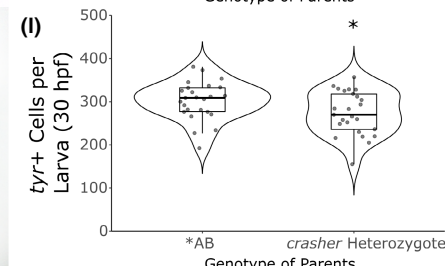
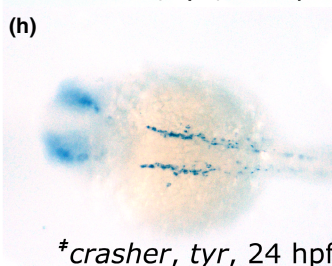
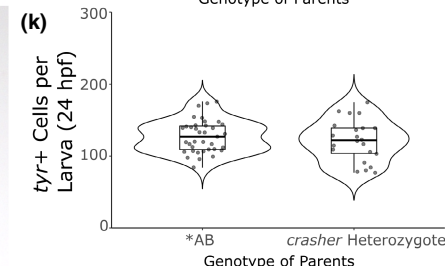
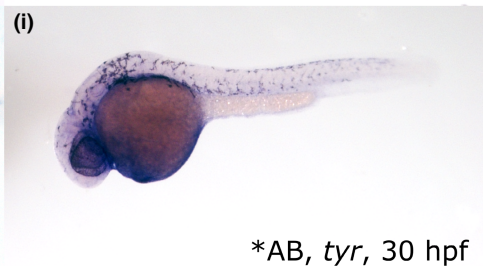
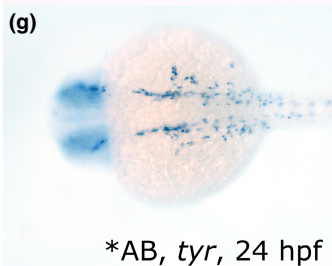
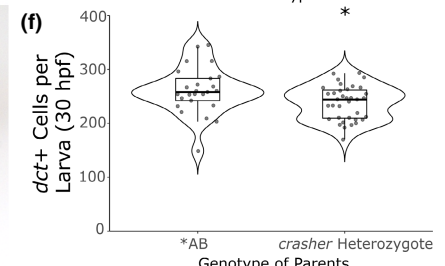
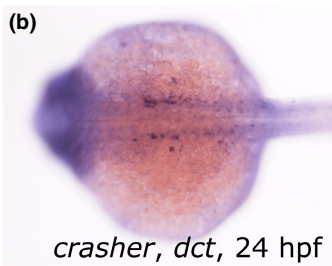
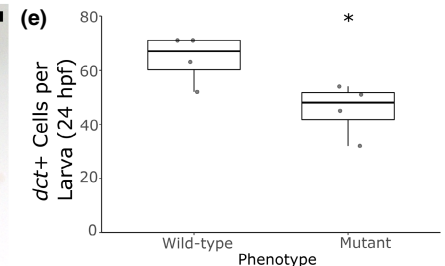
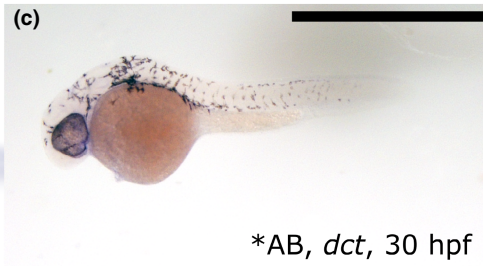
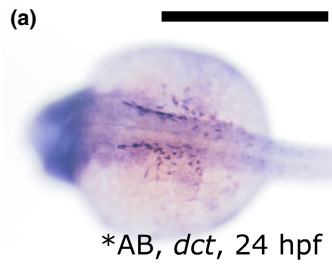
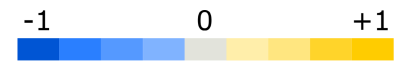


FIGURE 4 Specification and early differentiation markers are unchanged in *crasher* (*ap3d1* mutants). (a and b) Melanoblast/iridoblast bipotent precursor marker, *foxd3*, expression is unchanged in progeny of *crasher* heterozygotes. (c–h) *mitfa* expression is not altered in *crasher* heterozygote progeny. Melanoblast marker, *mitfa*, expression at 24 h postfertilization (hpf) in *AB control (c) and *crasher* heterozygote progeny (d) is not different. (e–h) Representative early differentiated melanophore marker, *mitfa*, expression at 30 hpf in *AB control (e) and *crasher* heterozygote progeny (f) from 2 replicates is not different. (g) *mitfa*+ cell counts are not significantly different for early differentiating melanophores at 30 hpf between progeny of *AB parents and *crasher* heterozygote parents (Student's *t*-test, $t(49) = 0.36$, $p = 0.72$). (h) *crasher* heterozygote progeny have similar *mitfa*+ signal, but less *mitfa*+ signal on the ventral side. Ratio is *mitfa*+ dorsal cell number divided by *mitfa*+ ventral cell number (Student's *t*-test, $t(45) = -0.94$, $p = 0.35$). Plots are violin box plots. Scale bars are 500 μm. Images labeled *crasher* are representative fish from the clutch.

FIGURE 5 Melanogenesis gene expression is reduced in *crasher* (*ap3d1*) mutants. (a, b and e) *dct* expression at 24 hpf is reduced in 1/4 of *crasher* heterozygote progeny (b) as assessed by a chi-square goodness-of-fit test to a 3 wild-type phenotype:1 mutant phenotype ratio ($\chi^2 = 1.08$, $\chi = 3.84$, $p = 0.30$). *dct*+ cell number is significantly reduced in mutant phenotype fish at 24 hpf (Student's *t*-test, $t[6] = 2.83$, $p = 0.03^*$). (c, d and f) *dct* expression is reduced in the *crasher* clutch overall by 30 cells on average at 30 hpf (Student's *t*-test, $t[6] = 2.39$, $p = 0.02^*$). (f) *crasher* clutch cell counts at 30 hpf segregate into a 3:1 ratio ($\chi^2 = 1.61$, $\chi = 3.84$, $p = 0.20$). (g–l) *tyr* is not significantly reduced at 24 hpf (Student's *t*-test, $t[57] = 0.90$, $p = 0.38$) (g, h and k), but is slightly reduced at 30 hpf in the *crasher* clutch (Student's *t*-test, $t[48] = 2.14$, $p = 0.04^*$) (i, j and l). (m–r) *tyrp1b*+ cells are reduced at 24 hpf in the *crasher* clutch (Student's *t*-test, $t[57] = 3.51$, $p = 8.73 \times 10^{-4}^{***}$), but no obvious mutant phenotype is observed (m, n and q). At 30 hpf, *tyrp1b*+ cells are significantly reduced (Student's *t*-test, $t[52] = 2.66$, $p = 0.01^{**}$), but no obvious mutant phenotype is observed (o, p, and r). (s) Expression heatmap of melanogenesis genes at 3 dpf using RNA-Seq. *tyrp1b* is reduced by >twofold (\log_2 fold difference of 1), while *dct* is also reduced. *tyr* expression is slightly increased. *mitfa* expression is not altered. (a, b, g, h, m and n) Scale bars are 500 μm. (c, d, i, j, o and p) Scale bars are 1 mm. *tyrp1b* 24 hpf and *tyr* 30 hpf experiment repeated twice. *dct* 30 hpf experiment repeated once. Plots are violin box plots. Images labeled *crasher* are representative fish from the clutch.



(s)



pigment cells. Candidate gene expression data did not reach a twofold change threshold; however, *crasher* mutants have reduced expression in *ap3d1* whole transcripts according to qRT-PCR (Figure 3a,b). Next, we asked if exon count in candidate gene mRNA was altered in the mutant. Reads mapping to each exon in each candidate gene in *crasher* and *AB showed the ratio of *crasher* reads per exon per gene was similar to *AB with the exception of a 5.5-fold increase in exon 14 of *ap3d1* in mutants (Figure 3c). CRISPR, RNA expression data, and mapping data supported *crasher* as an *ap3d1* mutant.

3.3 | Specification and early differentiation markers are not lost in *ap3d1* mutants

Using *in situ* hybridization, we examined neural crest and melanoblast specification markers, *foxd3* and *mitfa*, at 24 hpf (Curran et al., 2010). Because the mutant phenotype is not apparent until 2.5–3 dpf, we analyzed a clutch of 30 embryos from *crasher* (*ap3d1*) heterozygous parents, assuming one-quarter of the *crasher* clutch progeny would be homozygous recessive and cell count distributions would be bimodal (two separate violin plot peaks with one peak at third of the width of the other). *foxd3* and *mitfa* expression were similar between all progeny from *crasher* heterozygous parents and *AB fish suggesting specification was normal in *crasher* (Figure 4a–d).

We tested if melanophore differentiation failed in *crasher* mutants by examining differentiating *mitfa*⁺ melanophores at 30 hpf (Figure 4e–g). The *crasher* clutch had a greater proportion of fish with less signal distributed over the ventral side, but this was not statistically significant, nor were the differences in overall cell counts (Figure 4h). No obvious phenotype distinguishing one-quarter of the *crasher* clutch was observed.

3.4 | Melanogenesis gene expression is altered in *ap3d1* mutants

We asked if the *crasher* mutant's light melanophores resulted from reduced melanogenesis gene expression. Using *in situ* hybridization, we evaluated the expression of *tyr*, *dct*, and *tyrp1b* at 24 hpf and 30 hpf. *dct* expression was strongly reduced at 24 hpf in one-quarter of the *crasher* clutch. We performed a chi-squared goodness-of-fit test in which the null hypothesis was the ratio of wild-type phenotype fish to *crasher* phenotype fish was 3:1 (R Core Team, 2021). The null hypothesis was not rejected, and the test confirmed the ratio of wild-type phenotype fish to *crasher* phenotype fish was 3:1 (Figure 5a,b). *dct*⁺ cell number was reduced in *crasher* phenotype fish (Figure 5e). No obvious *crasher* phenotype stands out in *dct*⁺ expression at 30 hpf, though we observed an overall reduction in *dct*⁺ cell number in the *crasher* clutch (Figure 5c,d,f). However, the distribution of *dct*⁺ cells was different between the *AB clutch and *crasher* clutch. The lower grouping of cell counts appeared to form a separate group and matched a 3:1 ratio. This group did not have a distinct expression pattern like mutants at 24 hpf. *dct* expression is

possibly induced later in development in *crasher* mutants than their wild-type siblings, and mutants “catch up” slightly by 30 hpf. To our knowledge, there has not been a link between *dct* expression and *ap3d1* gene function before now.

tyr expression was examined, but a *crasher* phenotype was not readily observable in a quarter of the *crasher* clutch (Figure 5g–i). At 24 hpf, *tyr*⁺ cells were not reduced, and the distributions of these cell counts were not strongly bimodal (Figure 5k). At 30 hpf, overall

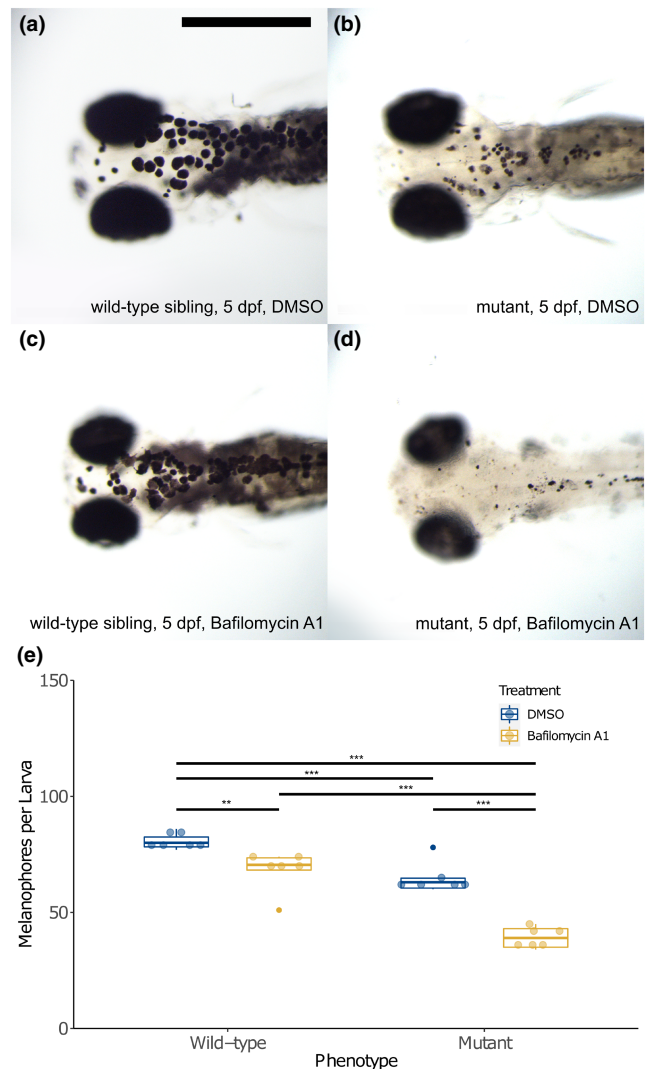


FIGURE 6 Autophagy inhibition with bafilomycin A1 negatively impacts melanophore survival in *crasher* (*ap3d1*) mutants. (a–d) Melanophore morphology of mutant fish treated with 50 nM bafilomycin A1 appears more punctate. (e) Melanophore count boxplot of *crasher* mutants and wild-type siblings treated with bafilomycin A1 or DMSO. Bafilomycin A1-treated mutants have 39.51% fewer melanophores ($\mu = 39.2$, $SD = 4.75$) than DMSO-treated mutants ($\mu = 64.8$, $SD = 6.76$). Bafilomycin A1-treated wild-type siblings have 15.74% fewer melanophores ($\mu = 68.0$, $SD = 8.70$) than DMSO-treated wild-type siblings ($\mu = 80.7$, $SD = 3.39$). (two-way ANOVA, phenotype $F(1, 20) = 77.03$, $p = 2.71 \times 10^{-8}$, treatment $F(1, 20) = 56.74$, $p = 2.92 \times 10^{-7}$, interaction $F(1, 20) = 6.53$, $p = 0.02$, Tukey HSD performed to determine group differences, $p < 0.001$ ***, $p < 0.01$ **, $p < 0.05$ *). Scale bar is 500 μm .

numbers of *tyr*+ cells are reduced, but we did not observe a distinct *crasher* mutant phenotype (Figure 5i,j,l).

No apparent mutant phenotype in *tyrp1b*+ cells was observed (Figure 5m–p). At 24 hpf, *tyrp1b*+ cells did not have a strong bimodal distribution in the *crasher* clutch. *tyrp1b*+ cell numbers at 24 hpf and 30 hpf were reduced overall in the *crasher* clutch (Figure 5q,r).

We pulled melanogenesis pathway expression data from our RNA-Seq dataset and compared expression levels between *AB fish and *crasher* mutants at 3 dpf (Figure 5s). *mitfa* is highly expressed in differentiated melanophores, and it was unchanged between *crasher* and *AB clutches, indicating melanophores were differentiating (Higdon et al., 2013). It is less likely changes in other melanogenesis genes are due to reduced melanophore number. *tyr* expression was slightly increased. This data is in contrast with our *in situ* data showing *crasher* clutches had fewer *tyr*+ cells at 30 hpf. *dct* expression at 3 dpf was decreased in mutants, and mutants had fewer *dct*+ cells at 24 hpf. *tyrp1b* expression was decreased to a larger degree at 3 dpf compared with *dct* expression which we did not observe in our *in situ* data at earlier timepoints. Taken together, *dct* and *tyrp1b* expression was most affected in *crasher* mutants.

3.5 | *ap3d1* promotes survival of melanophores via autophagy

The punctate, *crasher* melanophore morphology is similar to other pigment-deficient zebrafish mutants. Specifically, *vps11* mutants display fragmented cells similar to punctate cells in *crasher* mutants (Clancey et al., 2013). Autophagy was significantly upregulated in *crasher* mutants at 3 dpf according to Generally Applicable Gene-set Enrichment analysis of RNA-Seq data (Table S5; Figure S1). We hypothesized *crasher* mutants upregulate autophagy to maintain melanophore number because of the known role of autophagy in melanophore survival (Clancey et al., 2013). Therefore, inhibiting autophagy would reduce melanophore number in mutants. We treated mutants and WT siblings with autophagy-inhibitor, bafilomycin A1, starting at 2.5 dpf (Figure 6). At 5 dpf, we observed a ~39.51% decrease in dorsal and ventral stripe melanophores in mutants treated with bafilomycin compared to DMSO-treated mutants, and a 15.74% decrease in dorsal and ventral stripe melanophores in WT siblings treated with bafilomycin compared with DMSO-treated WT siblings (Figure 6a–e; Table S6). We suggest autophagy promotes melanophore survival when *ap3d1* is mutated.

4 | DISCUSSION

We characterized a novel syndromic albinism zebrafish model named *crasher*. Mutations in *ap3d1* caused aberrant pigmentation in zebrafish, as seen in HPS patients, *ap3d1* mutant mocha mice, and other melanogenesis enzyme trafficking zebrafish mutants, such as *vps11* (Ammann et al., 2016; Clancey et al., 2013; Kantheti et al., 1998). Among HPS10 animal models, *crasher* uniquely overexpressed exon

14 of *ap3d1*. Though the etiology of the allele is still unknown, it could be possible that exon 14 is left in a greater proportion of alternatively spliced transcripts in mutants than WT fish. Furthermore, the mutation may lie in a promoter as evidenced by reduced *ap3d1* expression, leading to decreased protein availability. Further studies will clarify the genetic nature of exon overexpression in *crasher* and its impact on *ap3d1* protein activity.

crasher mutants do not survive, and cause of death is unknown. Patients with HPS10 die of infection (Ammann et al., 2016; Mohammed et al., 2019). According to GAGE analysis, *crasher* showed decreased expression in ribosome, oxidative phosphorylation, proteasome, and cardiac muscle contraction pathways, possibly indicating systemic stress, but these pathway reductions require further mechanistic studies to determine their impact on organismal health (Table S5). Deficiencies in these pathways are not necessarily linked to syndromic albinism disorders. *crasher* mutants have upregulated immune signaling pathways which may not parallel the immune dysfunction observed in patients with HPS10 (Ammann et al., 2016; Mohammed et al., 2019). RNA-Seq was performed at 3 dpf, 6 to 8 days before mutants die, and may not reflect immune dysfunction present later.

Specified and early differentiated melanophores were not affected by *ap3d1* mutations. Melanogenesis was affected in *crasher* mutants, likely due to changes in the melanogenesis gene expression (*dct* and *tyrp1b*) in addition to melanogenesis enzyme trafficking defects (Richmond et al., 2005). AP-3 regulates zinc in mouse brains (Kantheti et al., 1998). DCT and TYRP1 rely on zinc as a cofactor, but whether AP-3 directly or indirectly mediates melanogenesis gene expression requires further investigation (Lai et al., 2017; Solano et al., 1996). Interestingly, LROs traffic mRNA cleavage protein, Ago. *Garnet* flies mutated in the AP-3 subunit delta have increased RNA silencing and decreased pigmentation (Harris et al., 2011). *crasher* is an attractive model to study *dct* and *tyrp1b* expression and cell trafficking effects on the expression of melanogenesis enzyme mRNA.

Autophagy is a cellular process involved in melanocyte loss and survival (Clancey et al., 2013). Inhibiting autophagy negatively impacted *crasher* melanophore survival, suggesting autophagy upregulation occurs to prevent further melanophore loss in *crasher*. The AP-3 complex may interact with PI(4)KII α , involved in autophagosome maturation, and ATG9A, an autophagy sorting signal, to transport cargo from the Golgi to the autophagosome (De Tito et al., 2020). If AP-3 is needed for autophagosome maturation, then loss of AP-3 would be expected to inhibit autophagy. However, AP-3 complex loss is associated with increased LC3-II activation in a cell specific manner, and LC3-II activation is correlated with autophagosome formation (Kabeya et al., 2000; Mantegazza et al., 2017). Additionally, treatment of *vps11* zebrafish mutants with bafilomycin A1 increases melanophore number, indicating autophagy and/or pH regulation play different roles during melanophore development (Clancey et al., 2013). Further studies on autophagy in *crasher* and *vps11* mutants are needed to understand the context in which autophagy impacts melanophore survival.

crasher is a novel zebrafish model for human HPS10. Whether mutants display the neurological and immunological symptoms in

HPS10 remains to be tested. In any case, *crasher* will be an excellent model to better understand AP-3 complex, specifically the δ subunit, function in pigment development and disease.

ACKNOWLEDGMENTS

Special thanks to the Johnson Lab (Washington University) for gifting the *crasher* mutant, the Raible Lab (University of Washington) for CRISPR training, Taylen Nappi for advice on qRT-PCR, and all Cooper lab members for care of zebrafish lines as well as support. This work was supported (in part) by the Poncin Scholarship Fund (awarded to S.J.N), Washington State University (WSU) Vancouver (awarded to C.D.C.), WSU College of Veterinary Medicine Intramural Funding Program (awarded to C.D.C), WSU College of Arts and Sciences (awarded to S.J.N.) and National Institutes of Health Grant HD103609 (awarded to C.D.C.). No conflicts of interest are reported.

DATA AVAILABILITY STATEMENT

The data that support the findings of this study are available from the corresponding author upon reasonable request.

REFERENCES

- Ammann, S., Schulz, A., Krägeloh-Mann, I., Dieckmann, N. M., Niethammer, K., Fuchs, S., Eckl, K. M., Plank, R., Werner, R., Altmüller, J., Thiele, H., Nürnberg, P., Bank, J., Strauss, A., von Bernuth, H., Zur Stadt, U., Grieve, S., Griffiths, G. M., Lehmborg, K., ... Ehl, S. (2016). Mutations in AP3D1 associated with immunodeficiency and seizures define a new type of Hermansky-Pudlak syndrome. *Blood*, 127, 997–1006. <https://doi.org/10.1182/blood-2015-09-67163>
- Andrews, S. (2019). Babraham Bioinformatics - FastQC a quality control tool for high throughput sequence data. Retrieved from <https://www.bioinformatics.babraham.ac.uk/projects/fastqc/>.
- Beirl, A. J., Linbo, T. H., Cobb, M. J., & Cooper, C. D. (2014). oca2 regulation of chromatophore differentiation and number is cell type specific in zebrafish. *Pigment Cell & Melanoma Research*, 27, 178–189. <https://doi.org/10.1111/pcmr.12205>
- Bolger, A. M., Lohse, M., & Usadel, B. (2014). Trimmomatic: A flexible trimmer for Illumina sequence data. *Bioinformatics (Oxford, England)*, 30(15), 2114–2120.
- Braasch, I., Scharl, M., & Volff, J. N. (2007). Evolution of pigment synthesis pathways by gene and genome duplication in fish. *BMC Evolutionary Biology*, 7, 74. <https://doi.org/10.1186/1471-2148-7-74>
- Braasch, I., Liedtke, D., Volff, J.-N., & Scharl, M. (2009). Pigmentary function and evolution of tyrp1 gene duplicates in fish. *Pigment Cell & Melanoma Research*, 22, 839–850. <https://doi.org/10.1111/j.1755-148X.2009.00614.x>
- Camp, E., & Lardelli, M. (2001). Tyrosinase gene expression in zebrafish embryos. *Development Genes and Evolution*, 211, 150–153.
- Clancey, L. F., Beirl, A. J., Linbo, T. H., & Cooper, C. D. (2013). Maintenance of melanophore morphology and survival is cathepsin and vps11 dependent in zebrafish. *PLoS One*, 8, e65096. <https://doi.org/10.1371/journal.pone.0065096>
- Curran, K., Lister, J. A., Kunkel, G. R., Prendergast, A., Parichy, D. M., & Raible, D. W. (2010). Interplay between Foxd3 and Mitf regulates cell fate plasticity in the zebrafish neural crest. *Developmental Biology*, 344, 107–118. <https://doi.org/10.1016/j.ydbio.2010.04.023>
- De Tito, S., Hervás, J. H., van Vliet, A. R., & Tooze, S. A. (2020). The Golgi as an assembly line to the autophagosome. *Trends in Biochemical Sciences*, 45, 484–496. <https://doi.org/10.1016/j.tibs.2020.03.010>
- Dobin, A., Davis, C. A., Schlesinger, F., Drenkow, J., Zaleski, C., Jha, S., Batut, P., Chaisson, M., & Gingeras, T. R. (2013). STAR: ultrafast universal RNA-seq aligner. In *STAR: Ultrafast universal RNA-seq aligner*. *Bioinformatics*. Oxford. <https://doi.org/10.1093/bioinformatics/bts635>
- Durinck, S., Moreau, Y., Kasprzyk, A., Davis, S., De Moor, B., Brazma, A., & Huber, W. (2005). BioMart and Bioconductor: A powerful link between biological databases and microarray data analysis. *Bioinformatics*, 21, 3439–3440. <https://doi.org/10.1093/bioinformatics/bti525>
- Federico, J. R., Krishnamurthy, K. (2020). Albinism. [Updated 2020 Aug 28]. In: StatPearls [Internet]. Treasure Island (FL): StatPearls Publishing; 2020 Jan. Available from: <https://www.ncbi.nlm.nih.gov/books/NBK519018/>
- Fox, J., & Weisberg, S. (2019). *An {R} companion to applied regression* (3rd ed.). Sage. <https://socialsciences.mcmaster.ca/jfox/Books/Companion/>
- Garrido, G., Fernández, A., & Montoliu, L. (2021). HPS11 and OCA8: Two new types of albinism associated with mutations in BLOC1S5 and DCT genes. *Pigment Cell & Melanoma Research*, 34, 10–12. <https://doi.org/10.1111/pcmr.12929>
- Gross, J. & Ligges, U. (2015). *nortest: Tests for normality*. R package version 1.0-4. <https://CRAN.R-project.org/package=nortest>
- Harris, D. A., Kim, K., Nakahara, K., Vásquez-Doorman, C., & Carthew, R. W. (2011). Cargo sorting to lysosome-related organelles regulates siRNA-mediated gene silencing. *The Journal of Cell Biology*, 194, 77–87. <https://doi.org/10.1083/jcb.201102021>
- Herrling, T., Jung, K., & Fuchs, J. (2008). The role of melanin as protector against free radicals in skin and its role as free radical indicator in hair. *Spectrochimica Acta. Part A, Molecular and Biomolecular Spectroscopy*, 69, 1429–1435. <https://doi.org/10.1016/j.saa.2007.09.030>
- Higdon, C. W., Mitra, R. D., & Johnson, S. L. (2013). Gene expression analysis of zebrafish melanocytes, iridophores, and retinal pigmented epithelium reveals indicators of biological function and developmental origin. *PLoS One*, 8, e67801. <https://doi.org/10.1371/journal.pone.0067801>
- Hoekstra, H. (2006). Genetics, development and evolution of adaptive pigmentation in vertebrates. *Heredity*, 97, 222–234. <https://doi.org/10.1038/sj.hdy.6800861>
- Howell, D. C. (2009). Permutation tests for factorial ANOVA designs. Retrieved from <https://www.uvm.edu/~statdhtx/StatPages/PermutationAnova/PermTestsAnova.html>
- Inena, G., Chu, B., Falay, D., Limengo, B., Matondo, I., Bokanga, A., Kovarik, C., & Williams, V. L. (2020). *Patterns of skin cancer and treatment outcomes for patients with albinism at Kisangani clinic*. Democratic Republic of Congo. <https://doi.org/10.1111/ijd.14988>
- Izquierdo, N. J., Townsend, W., & Hussels, I. E. (1995). Ocular findings in the Hermansky-Pudlak syndrome. *Transactions of the American Ophthalmological Society*, 93, 191. [https://doi.org/10.1016/s0002-9394\(14\)70555-0](https://doi.org/10.1016/s0002-9394(14)70555-0)
- Kabeya, Y., Mizushima, N., Ueno, T., Yamamoto, A., Kirisako, T., Noda, T., Kominami, E., Ohsumi, Y., & Yoshimori, T. (2000). LC3, a mammalian homologue of yeast Apg8p, is localized in autophagosomal membranes after processing. *The EMBO Journal*, 19, 5720–5728. <https://doi.org/10.1093/emboj/19.21.5720>
- Kantheti, P., Qiao, X., Diaz, M. E., Peden, A. A., Meyer, G. E., Carskadon, S. L., Kapfhamer, D., Sufalko, D., Robinson, M. S., Noebels, J. L., & Burmeister, M. (1998). Mutation in AP-3 delta in the mocha mouse links endosomal transport to storage deficiency in platelets, melanosomes, and synaptic vesicles. *Neuron*, 21, 111–122. [https://doi.org/10.1016/s0896-6273\(00\)80519-x](https://doi.org/10.1016/s0896-6273(00)80519-x)
- Kassambara, A. (2021). *rstatix: Pipe-friendly framework for basic statistical tests*. R package version 0.7.0. <https://CRAN.R-project.org/package=rstatix>

- Kawakami, A., & Fisher, D. E. (2017). The master role of microphthalmia-associated transcription factor in melanocyte and melanoma biology. Laboratory investigation; a journal of technical methods and pathology, *97*, 649–656. <https://doi.org/10.1038/labinvest.2017.9>
- Kelsh, R. N., Schmid, B., & Eisen, J. S. (2000). Genetic analysis of melanophore development in zebrafish embryos. *Developmental Biology*, *225*, 277–293. <https://doi.org/10.1006/dbio.2000.9840>
- Kimmel, C. B., Ballard, W. W., Kimmel, S. R., Ullmann, B., & Schilling, T. F. (1995). Stages of embryonic development of the zebrafish. *Developmental Dynamics: An Official Publication of the American Association of Anatomists*, *203*, 253–310. <https://doi.org/10.1002/aja.1002030302>
- Koboldt, D. C., Zhang, Q., Larson, D. E., Shen, D., McLellan, M. D., Lin, L., Miller, C. A., Mardis, E. R., Ding, L., & Wilson, R. K. (2012). VarScan 2: Somatic mutation and copy number alteration discovery in cancer by exome sequencing. *Genome Research*, *22*, 568–576. <https://doi.org/10.1101/gr.129684.111>
- Lai, X., Wichers, H. J., Soler-Lopez, M., & Dijkstra, B. W. (2017). Structure of Human Tyrosinase Related Protein 1 Reveals a Binuclear Zinc Active Site Important for Melanogenesis. *Angewandte Chemie (International ed. in English)*, *56*, 9812–9815. <https://doi.org/10.1002/anie.201704616>
- Li, H., Handsaker, B., Wysoker, A., Fennell, T., Ruan, J., Homer, N., Marth, G., Abecasis, G., Durbin, R., & 1000 Genome Project Data Processing Subgroup. (2009). The sequence alignment/map format and SAMtools. *Bioinformatics*, *25*, 2078–2079. <https://doi.org/10.1093/bioinformatics/btp352>
- Lister, J. A., Robertson, C. P., Lepage, T., Johnson, S. L., & Raible, D. W. (1999). Nacre encodes a zebrafish microphthalmia-related protein that regulates neural-crest-derived pigment cell fate. *Development*, *126*(17), 3757–3767.
- Luo, W., & Brouwer, C. (2013). Pathview: An R/Bioconductor package for pathway-based data integration and visualization. *Bioinformatics*, *29*, 1830–1831. <https://doi.org/10.1093/bioinformatics/btt285>
- Luo, W., Friedman, M. S., Shedden, K., Hankenson, K. D., & Woolf, P. J. (2009). GAGE: Generally applicable gene set enrichment for pathway analysis. *BMC Bioinformatics*, *10*, 1–17. <https://doi.org/10.1186/1471-2105-10-161>
- Mantegazza, A. R., Wynosky-Dolfi, M. A., Casson, C. N., Lefkovich, A. J., Shin, S., Brodsky, I. E., & Marks, M. S. (2017). Increased autophagic sequestration in adaptor protein-3 deficient dendritic cells limits inflammasome activity and impairs antibacterial immunity. *PLoS Pathogens*, *13*, e1006785. <https://doi.org/10.1371/journal.ppat.1006785>
- Mohammed, M., Al-Hashmi, N., Al-Rashdi, S., Al-Sukaiti, N., Al-Adawi, K., Al-Riyami, M., & Al-Maawali, A. (2019). Biallelic mutations in AP3D1 cause Hermansky-Pudlak syndrome type 10 associated with immunodeficiency and seizure disorder. *European Journal of Medical Genetics*, *62*, 103583. <https://doi.org/10.1016/j.ejmg.2018.11.017>
- Moreno-Mateos, M. A., Vejnár, C. E., Beaudoin, J. D., Fernandez, J. P., Mis, E. K., Khokha, M. K., & Giraldez, A. J. (2015). CRISPRscan: Designing highly efficient sgRNAs for CRISPR-Cas9 targeting in vivo. *Nature Methods*, *12*, 982–988. <https://doi.org/10.1038/nmeth.3543>
- Odenthal, J., & Nusslein-Volhard, C. (1998). Fork head domain genes in zebrafish. *Development Genes and Evolution*, *208*, 245–258. <https://doi.org/10.1007/s004270050179>
- Park, S., Morya, V. K., Nguyen, D. H., Singh, B. K., Lee, H. B., & Kim, E. K. (2015). Unrevealing the role of P-protein on melanosome biology and structure, using siRNA-mediated down regulation of OCA2. *Molecular and Cellular Biochemistry*, *403*, 61–71. <https://doi.org/10.1007/s11010-015-2337-y>
- Pfaffl, M. W. (2001). A new mathematical model for relative quantification in real-time RT-PCR. *Nucleic acids Research*, *29*(9), e45. <https://doi.org/10.1093/nar/29.9.e45>
- Pillaiyar, T., Manickam, M., & Namasivayam, V. (2017). Skin whitening agents: Medicinal chemistry perspective of tyrosinase inhibitors. *Journal of Enzyme Inhibition and Medicinal Chemistry*, *32*, 403–425. <https://doi.org/10.1080/14756366.2016.1256882>
- Pingault, V., Ente, D., Dastot-Le Moal, F., Goossens, M., Marlin, S., & Bondurand, N. (2010). Review and update of mutations causing Waardenburg syndrome. *Human Mutation*, *31*, 391–406. <https://doi.org/10.1002/humu.12111>
- R Core Team. (2021). R: A language and environment for statistical computing. R Foundation for Statistical Computing. <https://www.R-project.org/>
- Richmond, B., Huizing, M., Knapp, J., Koshoffer, A., Zhao, Y., Gahl, W. A., & Boissy, R. E. (2005). Melanocytes derived from patients with Hermansky-Pudlak syndrome types 1, 2, and 3 have distinct defects in cargo trafficking. *The Journal of Investigative Dermatology*, *124*, 420–427. <https://doi.org/10.1111/j.0022-202X.2004.23585.x>
- Solano, F., Jiménez-Cervantes, C., Martínez-Liarte, J. H., García-Borrón, J. C., Jara, J. R., & Lozano, J. A. (1996). Molecular mechanism for catalysis by a new zinc-enzyme, dopachrome tautomerase. *The Biochemical Journal*, *313*, 447–453. <https://doi.org/10.1042/bj3130447>
- Thisse, C., Thisse, B., Schilling, T. F., & Postlethwait, J. H. (1993). Structure of the zebrafish *snail1* gene and its expression in wild-type, spatial and no tail mutant embryos. *Development*, *119*, 1203–1215. <https://doi.org/10.1242/dev.119.4.1203>
- Vanhauwaert, S., Van Peer, G., Rihani, A., Janssens, E., Rondou, P., Lefever, S., De Paepe, A., Coucke, P. J., Speleman, F., Vandesompele, J., & Willaert, A. (2014). Expressed repeat elements improve RT-qPCR normalization across a wide range of zebrafish gene expression studies. *PLoS One*, *9*(10), e109091. <https://doi.org/10.1371/journal.pone.0109091>
- Wang, H., Wan, Y., Yang, Y., Li, H., Mao, L., Gao, S., Xu, J., & Wang, J. (2019). Novel compound heterozygous mutations in OCA2 gene associated with non-syndromic oculocutaneous albinism in a Chinese Han patient: A case report. *BMC Medical Genetics*, *20*, 130. <https://doi.org/10.1186/s12881-019-0850-7>
- Westerfield, M. (2007). *Zebrafish book: A guide for the laboratory use of zebrafish (Danio rerio)* (5th ed.). Inst Of Neuro Science.
- Wickham, H., Averick, M., Bryan, J., Chang, W., McGowan, L. D., François, R., Golemund, G., Hayes, A., Henry, L., Hester, J., Kuhn, M., Pedersen, T. L., Miller, E., Bache, S. M., Müller, K., Ooms, J., Robinson, D., Seidel, D. P., Spinu, V., ... Yutani, H. (2019). Welcome to the tidyverse. *Journal of Open Source Software*, *4*(43), 1686. <https://doi.org/10.21105/joss.01686>
- Wickham, H., Hester, J., & Chang, W. (2020). *devtools: Tools to make developing R packages easier*. R package version 2.3.2. <https://CRAN.R-project.org/package=devtools>
- Yates, A. D., Achuthan, P., Akanni, W., Allen, J., Allen, J., Alvarez-Jarreta, J., Amode, M. R., Armean, I. M., Azov, A. G., Bennett, R., Bhai, J., Billis, K., Boddu, S., Marugán, J. C., Cummins, C., Davidson, C., Dodiya, K., Fatima, R., Gall, A., ... Flicek, P. (2020). Ensembl 2020. *Nucleic Acids Research*, *48*, D682–D688. <https://doi.org/10.1093/nar/gkz966>

SUPPORTING INFORMATION

Additional supporting information can be found online in the Supporting Information section at the end of this article.

How to cite this article: Neuffer, S. J., Beltran-Cardona, D., Jimenez-Perez, K., Clancey, L. F., Brown, A., New, L., & Cooper, C. D. (2022). AP-3 complex subunit delta gene, *ap3d1*, regulates melanogenesis and melanophore survival via autophagy in zebrafish (*Danio rerio*). *Pigment Cell & Melanoma Research*, *35*, 495–505. <https://doi.org/10.1111/pcmr.13055>